



Superconductivity and the effects of pressure and structure in single-crystalline SrNi₂P₂

F. Ronning,¹ E. D. Bauer,¹ T. Park,^{1,2} S.-H. Baek,¹ H. Sakai,^{1,3} and J. D. Thompson¹

¹*Los Alamos National Laboratory, Los Alamos, New Mexico 87545, USA*

²*Department of Physics, Sungkyunkwan University, Suwon 440-746, Korea*

³*Advanced Science Research Center, Japan Atomic Energy Agency, Tokai, Ibaraki 319-1195, Japan*

(Received 26 January 2009; revised manuscript received 27 February 2009; published 6 April 2009)

Heat capacity, magnetic susceptibility, NMR, and resistivity of SrNi₂P₂ single crystals are presented, illustrating a purely structural transition at 325 K with no magnetism. Bulk superconductivity is found at 1.4 K. The magnitude of the transition temperature T_c , fits to the heat-capacity data, the small upper critical field $H_{c2} = 390$ Oe, and Ginzburg-Landau parameter $\kappa = 2.1$ suggest a conventional fully gapped superconductor. With applied pressure a second structural phase transition occurs which results in an 8% reduction in the c/a ratio of lattice parameters. We find that superconductivity persists into this high-pressure phase, although the transition temperature is monotonically suppressed with increasing pressure. Comparison of these Ni-P data as well as layered Fe-As and Ni-As superconductor indicates that reduced dimensionality can be a mechanism for increasing the transition temperature.

DOI: [10.1103/PhysRevB.79.134507](https://doi.org/10.1103/PhysRevB.79.134507)

PACS number(s): 74.10.+v, 74.25.Bt, 74.70.Dd, 74.62.-c

I. INTRODUCTION

There have long been attempts to identify structure-property relations in superconducting materials that help in the identification of the pairing mechanism and the enhancement of the superconducting transition temperature. The discovery of superconductivity at 26 K in LaFeAsO (Ref. 1) has stimulated much recent work in compounds containing T -Pn layers (T =transition metal and Pn=pnictide). The highest transition temperatures to date are found in the tetragonal ZrCuSiAs structure type [e.g., 55 K in SmFeAs(O,F) (Ref. 2)], and a correlation has been identified between the As-Fe-As bond angle and T_c .³ Clearly, structural tuning can have a very dramatic effect on superconducting transition temperatures and further structure-property relations are needed to help guide the discovery of higher transition temperatures.

Reasonably high transition temperatures also have been found in the ThCr₂Si₂ structure [i.e., 38 K in (Ba,K)Fe₂As₂].⁴ The ThCr₂Si₂ structure is stable for two different bonding configurations between the atoms in the Si position of neighboring Cr₂Si₂ planes. Either the atoms in the Si position are sufficiently far apart that they are in a nonbonding state or they are close enough together that they are bonding (typical of single bond distances).⁵ Consequently, depending on the elements in the tetragonal ThCr₂Si₂ structure, one can induce an isostructural volume collapse with either substitution or pressure.⁶⁻⁹ We will refer to the bonding configuration as the “collapsed tetragonal” structure. Due to the increased bonding between layers, it is natural to anticipate that the collapsed tetragonal phase will be electronically more three dimensional (i.e., Fermi velocity ratio v_x/v_z closer to 1) than the nonbonding configuration. With Fe₂As₂ planes, the ThCr₂Si₂ structure generally adopts a nonbonding configuration between As atoms from neighboring planes. One exception is that CaFe₂As₂ can be driven into the collapsed tetragonal state with pressure.¹⁰ Interestingly, while the homogeneous collapsed tetragonal state does not show signs of superconductivity down to 2 K,¹¹ by using different pressure mediums a structurally inhomogeneous scenario is

induced¹² which possesses an onset of superconductivity at 13 K.^{13,14} This poses the question of what is the role of the collapsed tetragonal phase (and dimensionality in general) for superconductivity.

We attempt to shed light on this question with a study of SrNi₂P₂. At ambient pressure, SrNi₂P₂ crystallizes in the large tetragonal state above 325 K with an interlayer P-P distance of 3.120 Å corresponding to a nonbonding condition.⁶ Below 325 K, the system undergoes an orthorhombic distortion ($Immm$ space group) with a buckling in the Ni₂P₂ planes causing the interlayer P-P distance to oscillate between 3.282 Å (nonbonding) and 2.452 Å (bonding). With NMR measurements we show that there is no magnetism associated with this transition. By applying pressure, the collapsed tetragonal state can be induced with slight pressure (4 kbar at room temperature).⁶ Here, we first identify that SrNi₂P₂ is a bulk superconductor at ambient pressure with $T_c = 1.4$ K. An analysis of the data is consistent with a fully gapped conventional superconductor. By applying pressure, we find that the transition temperature is suppressed by less than 50% upon entering the collapsed tetragonal state. Consequently, we conclude that the necessary conditions for superconductivity, namely, the ability to create an attractive interaction which can overcome the screened coulomb repulsion between two quasiparticles, can be satisfied in the “collapsed tetragonal” state to the transition-metal pnictides in the ThCr₂Si₂ structure. Furthermore, by expanding the cell so as to increase the c/a ratio superconductivity is enhanced.

II. EXPERIMENTAL

Large platelike single crystals of SrNi₂P₂ were grown in Sn flux following the general recipe described in Ref. 15. The starting materials in the ratio of Sr:Ni:P:Sn = 1.3:2:2.3:16 were placed in an alumina crucible and sealed under vacuum in a quartz tube. The contents were then heated to 600 °C for 4 h followed by 900 °C for 200 h. Subsequently the charge was cooled to 650 °C at a rate of

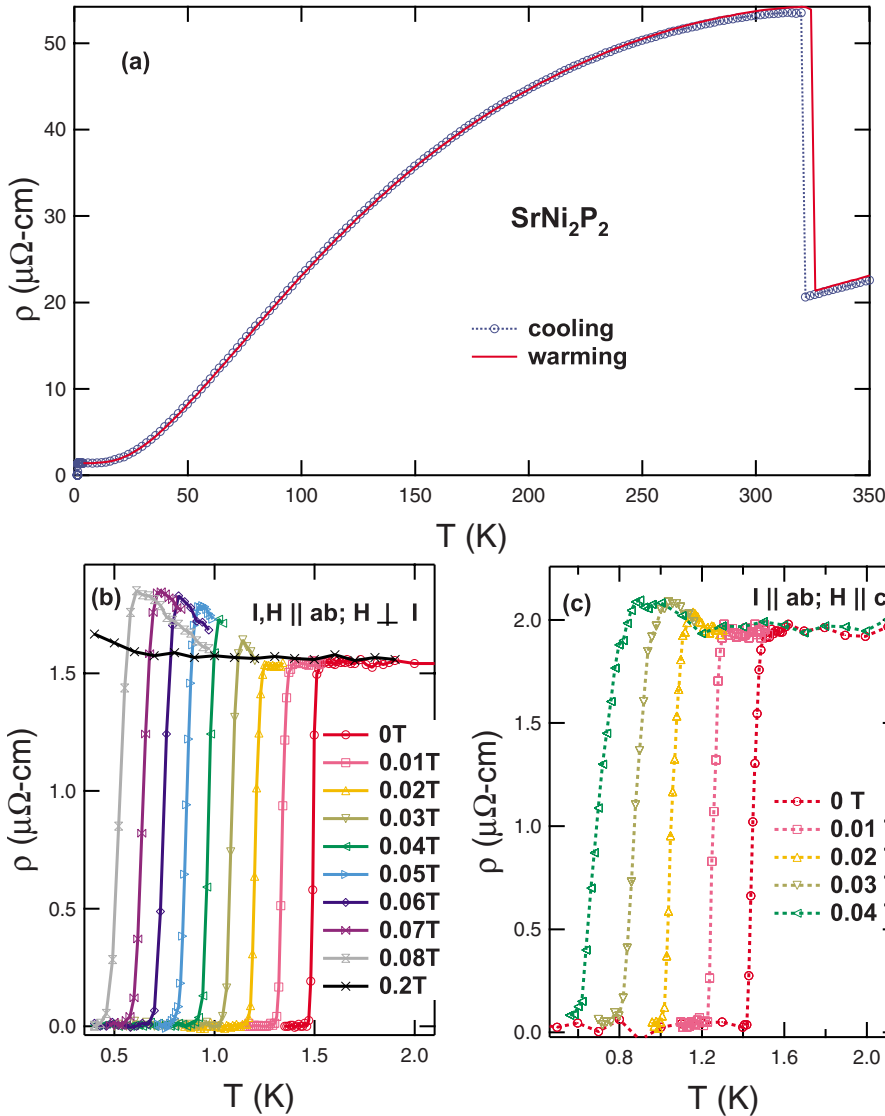


FIG. 1. (Color online) (a) In-plane electrical resistivity $\rho(T)$ ($I \parallel ab$) of SrNi_2P_2 for cooling and warming through the structural transition. (b) and (c) show the evolution of the superconducting transition for $H \parallel ab$ and $H \parallel c$, respectively.

3.5 °C/h at which point the excess Sn was spun off with the aid of a centrifuge. Powder x-ray diffraction confirms that the large platelike crystals with typical dimensions $5 \times 5 \times 0.2 \text{ mm}^3$ were SrNi_2P_2 .⁶

Specific-heat measurements were performed using an adiabatic relaxation technique in a Quantum Design PPMS. Resistance measurements were also performed in a Quantum Design PPMS using a linear research resistance bridge with an excitation current of 0.1 mA. Susceptibility measurements were performed in a Quantum Design MPMS with an applied field of 5 T. Results were in good agreement with data at 0.01 T, confirming that no ferromagnetic impurity contribution exists in the sample. ³¹P NMR was performed using a phase-coherent pulsed spectrometer. The external field was applied along the *c* axis.

For pressure measurements, a crystal was mounted inside a Teflon cup within a hybrid BeCu/NiCrAl clamp-type pressure cell with silicon oil as the pressure transmitting medium. The cup also contained a small piece of Pb whose known pressure-dependent superconducting transition¹⁶ enabled a determination of the pressure within the cell at low temperatures where the superconductivity is measured.

III. RESULTS

The in-plane resistivity of SrNi_2P_2 is shown in Fig. 1 and demonstrates a sharp first-order anomaly with thermal hysteresis associated with the structural transition previously observed in x-ray diffraction measurements.⁶ Here we find the transition occurs at 325 K upon warming and 320 K upon cooling. The first-order transition is further confirmed by magnetic-susceptibility measurements shown in Fig. 2. The susceptibility also shows the first-order transition at 325 K (upon warming) and 322 K (upon cooling). Interestingly, the susceptibility in the high-temperature phase is isotropic, but below the transition becomes anisotropic. While anisotropic *g* factors can result in an anisotropic Pauli susceptibility it is surprising that only the low-temperature phase shows this anisotropy.

To explore whether or not the susceptibility results could imply magnetic ordering or a changing magnetic moment coincident with the structural transition, we performed ³¹P NMR above and below the transition (see Fig. 3). The data above the transition show a very sharp double peak, indicative of very high crystallinity. Since only a single peak is

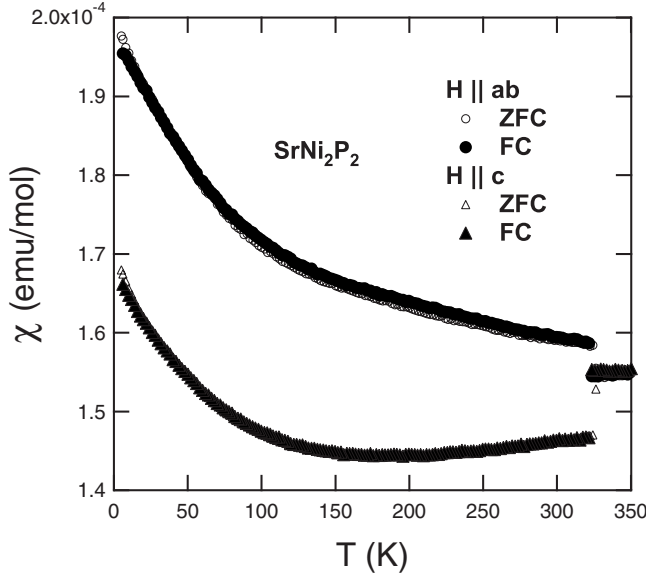


FIG. 2. Susceptibility of SrNi_2P_2 taken as a function of zero-field cooled (ZFC) and field cooled (FC) with an applied field of 5 T.

anticipated in the high-temperature ThCr_2Si_2 structure, the double peak at 332 K may be a consequence of either a slightly twinned sample or a small structural distortion possibly caused by thermally cycling through the structural transition. Upon lowering temperature through the transition, one sees that the central peak loses some intensity and a second double peak structure grows in at slightly higher frequencies. This is as expected on the basis of the structural transition alone for which there are now expected to be two inequivalent P positions populated in a ratio of 2:1.⁶ The fact that the central line does not shift or broaden at all implies that there is no internal field on the P sites which remain in the same crystallographic environment. Consequently, we can conclude that there is no magnetic order or a change in magnetic

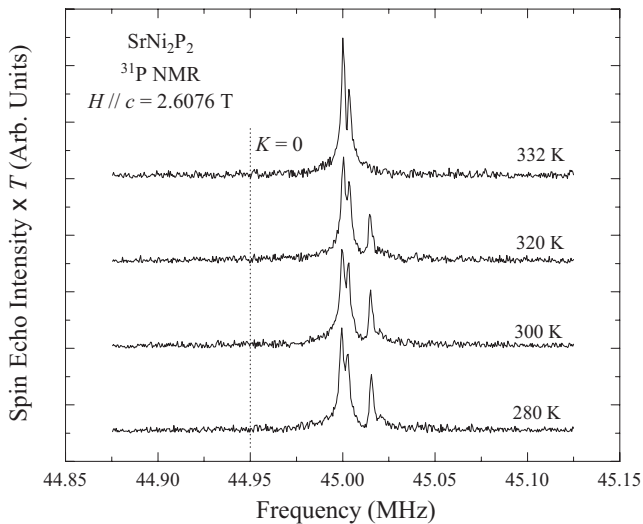


FIG. 3. ^{31}P NMR of SrNi_2P_2 on cooling through the structural transition illustrating the absence of magnetism. Dotted line represents the resonance line in the absence of a Knight shift K .

moment coincident with the structural transition at 325 K.

The resistivity below the structural transition is characteristic of a good metal with a residual resistivity ratio (RRR) $[\rho(300\text{ K})/\rho(4\text{ K})]$ of 40 and a residual resistivity of $1.8 \pm 0.2\ \mu\Omega\text{ cm}$. At 1.45 K the sample shows a sharp superconductivity as established by heat-capacity measurements shown below. With an applied magnetic field the superconducting transition is rapidly suppressed indicating a very small upper critical field. In addition, with an applied magnetic field there is a slight upturn in the resistivity before the superconducting transition. A similar feature has been observed in other iron-based pnictide superconductors and is discussed in Ref. 17.

Specific-heat data at low temperatures are shown in Fig. 4. A fit of the data (not shown) from 1.5 to 10 K to $C/T = \gamma + \beta T^2 + \delta T^4$ gives $\gamma = 15\text{ mJ/mol K}^2$ and $\beta = 0.23\text{ mJ/mol K}^4$, which implies a Debye temperature Θ_D of 348 K. Using a zero-temperature susceptibility of $\chi_0 = [2\chi_{ab}(2\text{ K}) + \chi_c(2\text{ K})]/3 = 1.86\text{ emu/mol}$, we find a Wilson ratio R_W of 0.9 using the expression $R_W = \pi^2 k_B^2 / 3 \mu_B^2 (\chi_0 / \gamma)$.

Bulk superconductivity is established by specific-heat measurements. By an equal area construction the specific heat gives a transition temperature of 1.415 K, consistent with the drop in resistivity. The fact that the low-temperature specific heat gives a jump $\Delta C / \gamma T_c = 1.27$ confirms the bulk nature of superconductivity. From BCS theory we expect the specific heat to be given by the formula

$$C_{\text{BCS}} = t \int_0^\infty dy \left(-\frac{6\gamma\Delta_0}{k_B\pi^2} \right) [f \ln f + (1-f)\ln(1-f)],$$

where $t = T/T_c$, $f = 1/[\exp(E/k_B T) + 1]$, $E = (\epsilon^2 + \Delta^2)^{1/2}$, $y = \epsilon/\Delta_0$, and $\Delta(T)/\Delta_0$ is taken from the tables of Mühlshlegel.¹⁸ The specific-heat curve, obtained by fixing $\gamma = 15\text{ mJ/mol K}^2$ from the high-temperature fit $T_c = 1.415\text{ K}$ and Δ_0 to the weak-coupling BCS value $= 1.76 k_B T_c$, is shown by the solid black curve in Fig. 4(b). Allowing the zero-temperature gap value Δ_0 to vary we obtain the dashed blue curve and find $\Delta_0 = 0.201\text{ meV} = 1.65 k_B T_c$. With the fitted curve to the specific heat, we can extract the condensation energy and equate it to the thermodynamic critical field giving $H_c = 185\text{ Oe}$. The reason that the best fit to the specific heat gives a value of Δ_0 below the weak-coupling value is uncertain, but may be caused by pair breaking impurities.¹⁹ We note that in several related superconductors the specific-heat jump is also slightly smaller than the weak-coupling BCS expectation of $\Delta C / \gamma T_c = 1.43$.²⁰⁻²⁴

As mentioned above, the upper critical fields of SrNi_2P_2 are small. In Fig. 5 we plot the upper critical field deduced from the midpoint of the resistive transition as well as the midpoint of the specific-heat curves. There is a slight anisotropy observed for the resistivity data. The upper critical field as determined by heat capacity is slightly lower, but surprisingly shows no anisotropy. The slope of the upper critical field from heat capacity is $dH_{c2}/dT_c = -0.039\text{ T/K}$. This gives an upper critical field of 390 Oe using

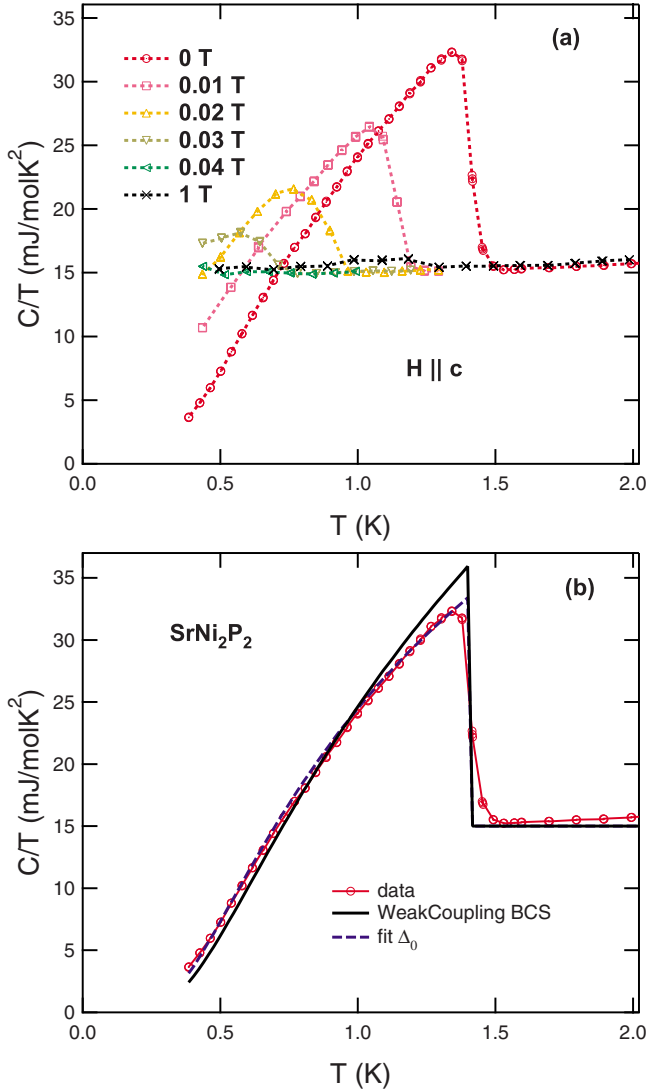


FIG. 4. (Color online) (a) Specific heat versus temperature for several magnetic fields applied in the plane of SrNi_2P_2 . (b) The zero-field heat-capacity data (circles) along with the theoretical expectation of the specific heat based on a purely weak-coupling BCS picture (solid black curve). Fit Δ_0 (dashed blue line) is a fit to the BCS expression holding $T_c=1.415 \text{ K}$, $\gamma=15 \text{ mJ/mol K}^2$ constant as described in the text.

the Werthamer-Helfand-Hohenberg (WHH) formula $H_{c2}^*(0) = -0.7T_c dH_{c2}/dT_c$ (Ref. 25) and a Ginzburg-Landau coherence length $\xi_{\text{GL}}=920 \text{ \AA}$ from the expression $H_{c2}(0) = \Phi_0/2\pi\xi_{\text{GL}}^2$, where $\Phi_0=2.07 \times 10^{-7} \text{ Oe cm}^2$ is the flux quantum. From the relations $H_c/H_{c1}=H_{c2}/H_c=\sqrt{2}\kappa = \sqrt{2}\lambda_{\text{eff}}/\xi_{\text{GL}}$, we extract $\kappa=2.1$, $H_{c1}=88 \text{ Oe}$, and $\lambda_{\text{eff}}=1935 \text{ \AA}$.

To investigate the influence of the crystal structure on superconductivity, we applied pressure to SrNi_2P_2 . At room temperature it is known that the orthorhombic structure transforms to a collapsed tetragonal structure at 4 kbar.^{6,8} Based on the pressure-temperature phase diagram for the structural collapse in CaFe_2As_2 (Ref. 11) we anticipate that at lower temperatures the structural transition to the “collapsed tetragonal” phase in SrNi_2P_2 will occur at pressures

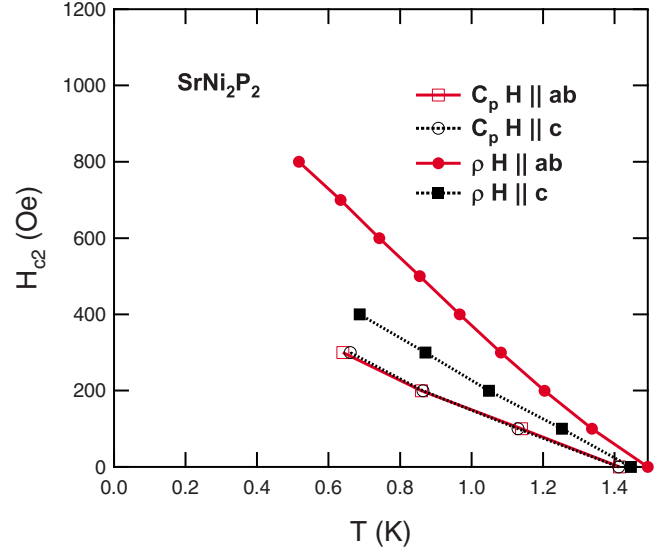


FIG. 5. (Color online) Superconducting phase diagram of SrNi_2P_2 as determined by the equal area construction of heat-capacity data and from the midpoint of the resistive transition.

less than 4 kbar. The structural transformation results in a volume change of -3.9% and a -8% change in the c/a ratio.⁸ Low-temperature resistivity is shown in Fig. 6(a). There is an immediate discontinuous change in the behavior from 0.5 to 2.9 kbar. The change in normal-state value of the resistivity likely reflects the change in structure which we anticipate with increasing pressure. The superconducting transition temperature decreases monotonically with pressure, although as shown in Fig. 6(b) there is a change in slope of T_c versus pressure upon entering the high-pressure phase. [At 25 kbar (not shown) there was no superconductivity observed down to 1.8 K.] At pressures above 4 kbar we suggest the system is structurally homogeneous, and thus our results show that the collapsed tetragonal phase of transition-metal pnictides in the ThCr_2Si_2 structure can support superconductivity.

IV. DISCUSSION

Several results from the ambient pressure data of SrNi_2P_2 are suggestive of a fully gapped BCS superconductor, including the fit to the heat-capacity data, the small value of H_{c2} , and κ . Band-structure calculations for SrNi_2P_2 give a density of states $N(E_F)=43 \text{ states/Ry cell}$.^{9,26} This gives an electron-boson renormalization $\lambda=1.02$, from the expression $\gamma=\pi^2k_B^2N(E_F)(1+\lambda)/3$, using the experimentally measured $\gamma=15 \text{ mJ/mol K}^2$. This is certainly sufficient to explain superconductivity in an electron-phonon pairing scenario. For example, using the simplified McMillan formula²⁷

$$T_c = \frac{\Theta_D}{1.45} \exp \left[- \frac{1.04(1+\lambda)}{\lambda - \mu^*(1+0.62\lambda)} \right]$$

and a very conservative estimate of $\mu^*=0.3$ gives $T_c=4.5 \text{ K}$. Furthermore, calculations show that BaNi_2P_2 has a larger density of states ($\gamma^{\text{th}}=9.32 \text{ mJ/mol K}^2$) (Ref. 9)

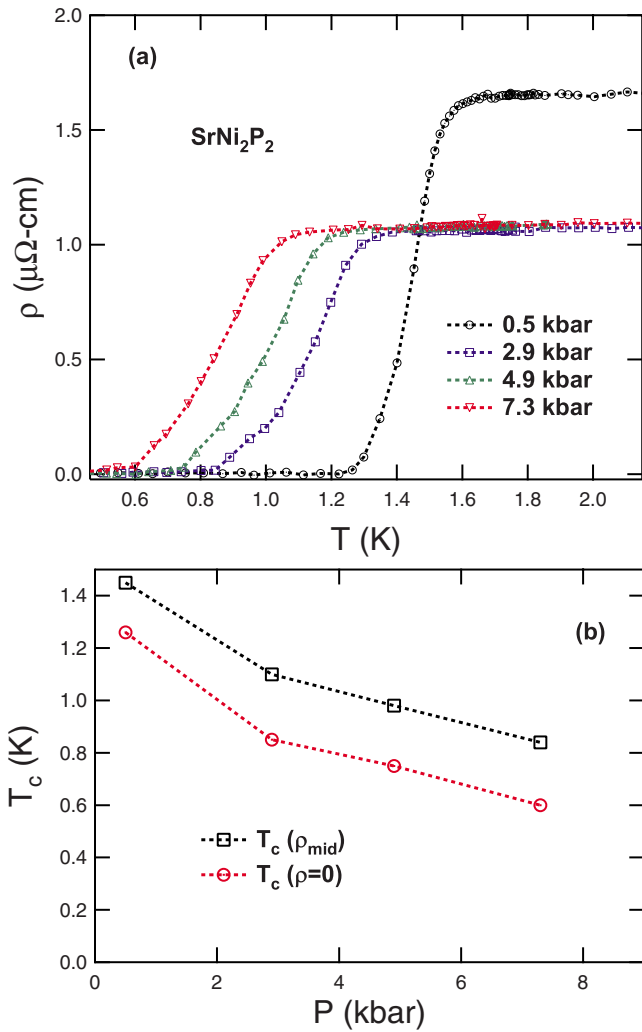


FIG. 6. (Color online) (a) Resistivity versus temperature of SrNi_2P_2 for several applied pressures. (b) T_c as a function of pressure as determined by the resistivity in (a) from both the midpoint of the transition (black squares) and the zero resistance state (red circles).

which is consistent with its larger superconducting transition temperature ($T_c=2.7$ K).²⁸ In addition, low-temperature thermal-conductivity data provide compelling evidence for fully gapped superconductivity in the related material BaNi_2As_2 .²¹ While not definitive, the accumulation of evidence suggests that SrNi_2P_2 is a conventional BCS superconductor.

An open question is whether the pairing mechanisms of the Fe-based systems and the Ni-based compounds are related. On the basis of band-structure calculations it has been argued that both $T=\text{Fe}$ and $T=\text{Ni}$ lie close to a magnetic instability,²⁹ however it remains the case that none of the Ni-based systems possess superconducting transition temperatures in excess of 5 K (Refs. 20, 22, 23, 28, and 30–37) nor do they have evidence for magnetism. Density functional calculations suggest that the two systems have unrelated pairing mechanisms based on the fact that they are unable to reproduce the high transition temperatures of the Fe-based compounds.^{38,39} However, it remains a possibility that the

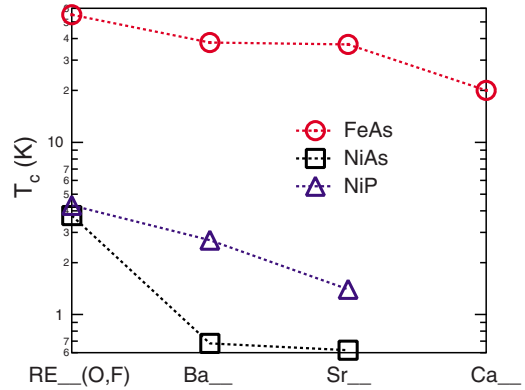


FIG. 7. (Color online) (a) Superconducting transition temperature across a few families of compounds for FeAs, NiAs, and NiP planes. For the FeAs series, T_c for $\text{SmFeAs}(\text{O},\text{F})$ and for hole doping on the Ba, Sr, Ca site was chosen (Refs. 2, 4, 41, and 42, respectively). T_c for the NiP and NiAs were taken from Refs. 31 and 28, this work, and Refs. 33, 20, and 22, respectively.

pairing mechanisms of the Ni-based systems are merely not as optimized for superconductivity as their iron-based cousins.

It is rather remarkable that superconductivity has been found in many of the nickel analogs for which the iron-based pnictide compounds also superconducts. Figure 7 shows that even the trend of the maximum superconducting transition temperature decreases monotonically from $\text{ReX}(\text{O},\text{F})$ to BaX_2 to SrX_2 to CaX_2 irrespective of whether $X=\text{FeAs}$, NiAs, or NiP. A possible interpretation of this trend is that T_c is suppressed with increasing dimensionality or, in other words, as the electronic structure becomes more isotropic. Comparison between the ZrCuSiAs and ThCr_2Si_2 structure types has already established that the electronic structure of the systems in the ThCr_2Si_2 structure are more three dimensional than those in the ZrCuSiAs structure.⁴⁰ Within the ThCr_2Si_2 structure this can be further understood from the decreasing ionic radius in going from Ba to Sr to Ca.^{5,9} Consequently, the pnictide atoms are closer together allowing for stronger hybridization along the c axis. Eventually the decreasing pnictide-pnictide distance will lead to the collapsed tetragonal state where the interlayer pnictides adopt a bonding configuration, which should be the most three dimensional due to the increased P-P hybridization along the z direction, and hence the least favorable for superconductivity. Our results, which show that superconductivity in SrNi_2P_2 is suppressed upon entering the collapsed tetragonal phase, further support the notion that increased three dimensionality found in the collapsed tetragonal state at higher pressures is detrimental for superconductivity. Further work is needed to determine how precisely dimensionality in terms of structural, magnetic, and electronic anisotropies influences the correlation between families observed in Fig. 7. Irrespective of the origin of the trend, this work suggests that CaNi_2P_2 and CaNi_2As_2 will be superconducting at temperatures below 1.4 and 0.62 K, respectively.

V. CONCLUSION

In conclusion, by ^{31}P NMR we have demonstrated the lack of magnetism in SrNi_2P_2 . We have also shown that SrNi_2P_2 is a bulk superconductor at ambient pressure at 1.4 K. Upon entering the collapsed tetragonal phase with applied pressure, the superconducting transition temperature is monotonically suppressed. Further work is necessary to determine whether SrNi_2P_2 under pressure is the first transition-metal pnictide in the ThCr_2Si_2 structure to possess bulk superconductivity or whether a similar unknown

mechanism as occurs in CaFe_2As_2 is at play. The suppression of T_c with pressure and across families of compounds demonstrates the notion that increased two dimensionality is a mechanism through which higher T_c 's can be achieved.

ACKNOWLEDGMENTS

We thank M. Graf for helpful comments. Work at Los Alamos National Laboratory was performed under the auspices of the U.S. Department of Energy.

- ¹Y. Kamihara, T. Watanabe, M. Hirano, and H. Hosono, *J. Am. Chem. Soc.* **130**, 3296 (2008).
- ²Z.-A. Ren, W. Lu, J. Yang, W. Yi, X.-L. Shen, Z.-C. Li, G.-C. Che, X.-L. Dong, L.-L. Sun, F. Zhou, and Z.-X. Zhou, *Chin. Phys. Lett.* **25**, 2215 (2008).
- ³C.-H. Lee, T. Ito, A. Iyo, H. Eisaki, H. Kito, M. T. Fernandez-Diaz, K. Kihou, H. Matsuhata, M. Braden, and K. Yamada, *J. Phys. Soc. Jpn.* **77**, 083704 (2008).
- ⁴M. Rotter, M. Tegel, and D. Johrendt, *Phys. Rev. Lett.* **101**, 107006 (2008).
- ⁵R. Hoffmann and C. Zheng, *J. Phys. Chem.* **89**, 4175 (1985).
- ⁶V. Keimes, D. Johrendt, A. Mewis, C. Huhnt, and W. Schlabitz, *Z. Anorg. Allg. Chem.* **623**, 1699 (1997).
- ⁷V. Keimes, A. Hellmann, D. Johrendt, A. Mewis, and Th. Woike, *Z. Anorg. Allg. Chem.* **624**, 830 (1998).
- ⁸C. Huhnt, W. Schlabitz, A. Wurth, A. Mewis, and M. Reehuis, *Phys. Rev. B* **56**, 13796 (1997).
- ⁹I. B. Shameem Banu, M. Rajagopalan, M. Yousuf, and P. Shenbagaraman, *J. Alloys Compd.* **288**, 88 (1999).
- ¹⁰A. Kreyssig, M. A. Green, Y. Lee, G. D. Samolyuk, P. Zajdel, J. W. Lynn, S. L. Budko, M. S. Torikachvili, N. Ni, S. Nandi, J. B. Leao, S. J. Poulton, D. N. Argyriou, B. N. Harmon, R. J. McQueeney, P. C. Canfield, and A. I. Goldman, *Phys. Rev. B* **78**, 184517 (2008).
- ¹¹W. Yu, A. A. Aczel, T. J. Williams, S. L. Budko, N. Ni, P. C. Canfield, and G. M. Luke, *Phys. Rev. B* **79**, 020511(R) (2009).
- ¹²A. I. Goldman, A. Kreyssig, K. Prokes, D. K. Pratt, D. N. Argyriou, J. W. Lynn, S. Nandi, S. A. J. Kimber, Y. Chen, Y. B. Lee, G. Samolyuk, J. B. Leao, S. J. Poulton, S. L. Budko, N. Ni, P. C. Canfield, B. N. Harmon, and R. J. McQueeney, *Phys. Rev. B* **79**, 024513 (2009).
- ¹³T. Park, E. Park, H. Lee, T. Klimczuk, E. D. Bauer, F. Ronning, and J. D. Thompson, *J. Phys.: Condens. Matter* **20**, 322204 (2008).
- ¹⁴M. S. Torikachvili, S. L. Budko, N. Ni, and P. C. Canfield, *Phys. Rev. Lett.* **101**, 057006 (2008).
- ¹⁵R. Marchand and W. Jeitschko, *J. Solid State Chem.* **24**, 351 (1978).
- ¹⁶A. Eiling and J. S. Schilling, *J. Phys. F: Met. Phys.* **11**, 623 (1981).
- ¹⁷J. G. Analytis, J.-H. Chu, A. S. Erickson, C. Kucharczyk, A. Serafin, A. Carrington, C. Cox, S. M. Kauzlarich, H. Hope, and I. R. Fisher, arXiv:0810.5368 (unpublished).
- ¹⁸B. Mühlischlegel, *Z. Phys.* **155**, 313 (1959).
- ¹⁹See, e.g., chapter by K. Maki and R. D. Parks, *Superconductivity* (Marcel Dekker, New York, 1969).
- ²⁰F. Ronning, N. Kurita, E. D. Bauer, B. L. Scott, T. Park, T. Klimczuk, R. Movshovich, and J. D. Thompson, *J. Phys.: Condens. Matter* **20**, 342203 (2008).
- ²¹N. Kurita, F. Ronning, Y. Tokiwa, E. D. Bauer, A. Subedi, D. J. Singh, J. D. Thompson, and R. Movshovich, arXiv:0811.3426, *Phys. Rev. Lett.* (to be published).
- ²²E. D. Bauer, F. Ronning, B. L. Scott, and J. D. Thompson, *Phys. Rev. B* **78**, 172504 (2008).
- ²³T. Klimczuk, T. M. McQueen, A. J. Williams, Q. Huang, F. Ronning, E. D. Bauer, J. D. Thompson, M. A. Green, and R. J. Cava, *Phys. Rev. B* **79**, 012505 (2009).
- ²⁴S. Kasahara, H. Fujii, H. Takeya, T. Mochiku, A. D. Thakur, and K. Hirata, *J. Phys.: Condens. Matter* **20**, 385204 (2008).
- ²⁵N. R. Werthamer, E. Helfand, and P. C. Hohenberg, *Phys. Rev.* **147**, 295 (1966).
- ²⁶The calculations of Ref. 9 were performed for an idealized tetragonal form of the structure which neglects the tripling of the size of the unit cell caused by a superstructure of the P position observed in the low-temperature structure by Ref. 6.
- ²⁷W. L. McMillan, *Phys. Rev.* **167**, 331 (1968).
- ²⁸T. Mine, H. Yanagi, T. Kamiya, Y. Kamihara, M. Hirano, and H. Hosono, *Solid State Commun.* **147**, 111 (2008).
- ²⁹G. Xu, W. Ming, Y. Yao, X. Dai, S.-C. Zhang, and Z. Fang, *Europhys. Lett.* **82**, 67002 (2008).
- ³⁰T. Watanabe, H. Yanagi, T. Kamiya, Y. Kamihara, H. Hiramatsu, M. Hirano, and H. Hosono, *Inorg. Chem.* **46**, 7719 (2007).
- ³¹M. Tegel, D. Bichler, and D. Johrendt, *Solid State Sci.* **10**, 193 (2008).
- ³²T. Watanabe, H. Yanagi, Y. Kamihara, T. Kamiya, M. Hirano, and H. Hosono, *J. Solid State Chem.* **181**, 2117 (2008).
- ³³L. Fang, H. Yang, P. Cheng, X. Zhu, G. Mu, and H.-H. Wen, *Phys. Rev. B* **78**, 104528 (2008).
- ³⁴Z. Li, G. F. Chen, J. Dong, G. Li, W. Z. Hu, D. Wu, S. K. Su, P. Zheng, T. Xiang, N. L. Wang, and J. L. Luo, *Phys. Rev. B* **78**, 060504(R) (2008).
- ³⁵J. Ge, S. Cao, and J. Zhang, arXiv:0807.5045 (unpublished).
- ³⁶V. L. Kozhevnikov, O. N. Leonidova, A. L. Ivanovskii, I. R. Shein, B. N. Goshchitskii, and A. E. Karkin, *JETP Lett.* **87**, 649 (2008).
- ³⁷H. Fujii and S. Kasahara, *J. Phys.: Condens. Matter* **20**, 075202 (2008).
- ³⁸A. Subedi, D. J. Singh, and M. H. Du, *Phys. Rev. B* **78**, 060506(R) (2008).
- ³⁹A. Subedi and D. J. Singh, *Phys. Rev. B* **78**, 132511 (2008).

⁴⁰M. A. Tanatar, N. Ni, C. Martin, R. T. Gordon, H. Kim, V. G. Kogan, G. D. Samolyuk, S. L. Budko, P. C. Canfield, and R. Prozorov, *Phys. Rev. B* **79**, 094507 (2009).

⁴¹K. Sasmal, B. Lv, B. Lorenz, A. M. Guloy, F. Chen, Y. Y. Xue,

and C. W. Chu, *Phys. Rev. Lett.* **101**, 107007 (2008).

⁴²G. Wu, H. Chen, T. Wu, Y. L. Xie, Y. J. Yan, R. H. Liu, X. F. Wang, J. J. Ying, and X. H. Chen, *J. Phys.: Condens. Matter* **20**, 422201 (2008).